Larval Morphology of Megaporus Brinck, 1943 (Coleoptera: Dytiscidae): Descriptions of M. Hamatus (Clark, 1862) and M. Gardnerii (Clark, 1862) and Phylogenetic Considerations

Authors: Alarie, Yves, Michat, Mariano C., and Watts, Chris H. S.

Source: The Coleopterists Bulletin, 74(1) : 139-160

Published By: The Coleopterists Society

URL: https://doi.org/10.1649/0010-065X-74.1.139

The Coleopterists Bulletin, 74(1): 139–160. 2020.

Larval Morphology of *Megaporus* Brinck, 1943 (Coleoptera: Dytiscidae): Descriptions of *M. hamatus* (Clark, 1862) and *M. gardnerii* (Clark, 1862) and Phylogenetic Considerations

Yves Alarie
Department of Biology, Laurentian University
Sudbury, Ontario, P3E 2C6, CANADA
yalarie@laurentian.ca

Mariano C. Michat
Laboratory of Entomology, DBBE-FCEN and IBBEA-CONICET
University of Buenos Aires, Buenos Aires, ARGENTINA

AND

Chris H. S. Watts
South Australian Museum, North Terrace, Adelaide, SA 5000, Australia

Abstract

The larvae of the Australian endemic species *Megaporus gardnerii* (Clark, 1862) and *M. hamatus* (Clark, 1862) are described and illustrated for the first time, with detailed morphometric and chaetotaxic analyses of the cephalic capsule, head appendages, legs, last abdominal segment, and urogomphi. We explore implications for understanding the evolution of larval morphological traits amongst selected Sternopriscina genera. A parsimony analysis based on 84 larval characteristics of seven species in five genera was conducted using the program TNT. Larvae of *Megaporus* Brinck are characterized by the primary seta AB3 articulated distad of seta AB2, a very elongate siphon, and predominantly elongate and hair-like secondary setae on the urogomphi. *Megaporus* is postulated to be closely related phylogenetically to *Chostonectes* Sharp in the context of this study, which reinforces previous hypotheses based on adult and molecular data sets. These results provide a phylogenetic framework for future studies of the larvae of the Sternopriscina.

Key Words: larvae, phylogeny, Sternopriscina, Australasia, Hydroporinae

DOI.org/10.1649/0010-065X-74.1.139

Introduction

Megaporus Brinck, 1943 is an Australasian endemic genus comprised of 11 species distributed throughout Australia, including Tasmania, and in New Guinea and New Caledonia (Miller and Bergsten 2016; Nilsson and Hájek 2019; Watts 1978). These beetles are found in a large number of aquatic habitats, but especially in ponds and stream margins with vegetation. In term of classification, *Megaporus* is included in the strictly Australasian hydroporine radiation Sternopriscina (ca. 155 spp. in 11 genera) (Nilsson and Hájek 2019) and is deemed closely related to *Chostonectes* Sharp, 1882 (Balke 1995; Hendrich *et al.* 2014; Miller and Bergsten 2014; Toussaint *et al.* 2015).

While still scanty, knowledge about larval morphology of members of the subtribe Sternopriscina has made good progress recently. Larvae of *Antiporus* Sharp, 1882 (Alarie and Watts 2004), *Paroster* Sharp, 1882 (Alarie *et al.* 2009), *Barretthydrus* Lea, 1927 (Alarie *et al.* 2018), and *Chostonectes* (Alarie *et al.* 2019) have been described according to the now-generalized larval descriptive format of Hydradephaga, which incorporates chaetotaxic analysis.

The discovery of the larvae of both *Megaporus gardnerii* (Clark, 1862) and *M. hamatus* (Clark, 1862), therefore, provided the impetus for this study, which has the following two goals: (1) to describe in detail the larvae of *Megaporus* including chaetotaxy analysis of the head capsule and appendages, legs, last abdominal segment and urogomphi, and (2) to compare in a phylogenetic context larval features of *Megaporus* with those of other associated Sternopriscina genera for which the larvae have been described comprehensively.

Material and Methods

Preparation and Observation. The descriptions of the larval stages and the taxonomic conclusions reported in this paper are based on the examination of larvae co-occurring with adults. Larvae were

disarticulated and mounted on standard glass slides in Hoyer's medium. Microscopic examination at magnifications of 80–800× was done using an Olympus BX50 compound microscope equipped with Nomarsky differential interference optics. Figures were prepared through use of a drawing tube attached to the microscope. Drawings were scanned and digitally inked using an Intuos 4 professional pen tablet (Wacom Co., Ltd. Kazo, Saitama, Japan). Voucher specimens are deposited in the larval collection of Y. Alarie (Department of Biology, Laurentian University, Canada).

Measurements. All measurements were made with a compound microscope equipped with a micrometer eyepiece. The part to be measured was adjusted so that it was, as nearly as possible, parallel to the plane of the objectives. We employed, with minimal modifications and additions, the terms used in previous papers dealing with larval morphology of the Sternopriscina (Alarie *et al.* 2009, 2018, 2019; Alarie and Watts 2004). The following measurements were taken. Head length (HL): total head length including the frontoclypeus, measured medially along epicranial stem. Head width (HW): maximum head width. Length of frontoclypeus (FRL): from apex of nasale to posterior margin of ecdysial suture. Occipital foramen width (OCW): maximum width measured along dorsal margin of occipital foramen. Length of mandible (MN): measured from laterobasal angle to apex. Width of MN: maximum width measured at base. Length of antenna (A), maxillary (MP) and labial (LP) palpi were derived by adding the lengths of the individual segments; each segment is denoted by the corresponding letter(s) followed by a number (e.g., A1: first antennomere), and A3' is used as an abbreviation for the apical lateroventral process of third antennomere. Length of leg (L) including the longest claw (C) was derived by adding the lengths of the individual segments; each leg is denoted by the letter L followed by a number (e.g., L1: prothoracic leg). Length of trochanter includes only the proximal portion and the length of the distal portion is included in the femoral length. Dorsal length (LASD) and ventral length (LASV) of last abdominal segment (LAS): measured along midline from anterior to posterior margin. Length of urogomphus (U) was derived by adding the lengths of the individual segments; each segment is denoted by the letter U followed by a number (e.g., U1: first urogomphomere). These measurements were used to calculate several ratios, which characterize the body shape.

Chaetotaxic analysis. Primary (observed in instar I) and secondary (added throughout the ontogenetic development) setae and pores were distinguished on the cephalic capsule, head appendages, legs, last abdominal segment, and urogomphus. The setae and pores were coded according to the system proposed by Alarie (1991) and Alarie and Michat (2007a) for the cephalic capsule and head appendages, Alarie *et al.* (1990) for the legs, and Alarie and Harper (1990) for the last abdominal segment and urogomphi. Setae are coded by two capital letters corresponding to the first two letters of the name of the structure on which the seta is located (AB, abdominal segment VIII; AN, antenna; CO, coxa; FE, femur; FR, frontoclypeus; LA, labium; MN, mandible; MX, maxilla; PA, parietale; TA, tarsus; TI, tibia; TR, trochanter; UR, urogomphus) and a number. Pores are coded in a similar manner except that the number is replaced by a lower-case letter. The position of the sensilla is described by adding the following abbreviations: A, anterior; AD, anterodorsal; AV, anteroventral; D, dorsal; PD, posterodorsal; Pr, proximal; PV, posteroventral.

Color. Description of color is given from ethanol-preserved specimens.

Phylogenetic analysis. To examine the phylogenetic signal of the larval characters of *Megaporus* and to test the relationships of this genus with other Sternopriscina, a cladistic analysis including seven species of Sternopriscina (five genera) and five species of other tribes of the Hydroporinae was conducted. The genera *Laccornis* Gozis, 1914 (tribe Laccornini), *Laccornellus* Roughley and Wolfe, 1987, *Canthyporus* Zimmermann, 1919 (tribe Laccornellini), *Celina* Aubé, 1837 (tribe Methlini), and *Hydrovatus* Motschulsky, 1853 (tribe Hydrovatini), which are generally recognized as ancestral lineages within the subfamily Hydroporinae based on adults (Miller *et al.* 2006; Roughley and Wolfe 1987), larvae (Alarie and Michat 2007b; Michat *et al.* 2007) and molecules (Miller and Bergsten 2014), were used as outgroups, rooting the tree with *Laccornis*. The analysis was performed using the program TNT (Goloboff *et al.* 2008). All characters were treated as unordered and equally weighted. An exact solution algorithm (implicit enumeration) was implemented to find the most parsimonious trees. Bremer support values were calculated using the commands 'hold 20000', 'sub n' and 'bsupport', where 'n' is the number of extra steps allowed. The process was repeated, increasing the length of the suboptimal cladograms by one step, until all Bremer values were obtained (Kitching *et al.* 1998). Bootstrap values were calculated using the following parameters: "standard (sample with replacement)"; 1000 replicates.

Results

Megaporus Brinck, 1943

(Figs. 1–19)

Diagnosis. Instar III of *Megaporus* can be distinguished from those of other genera of Australian

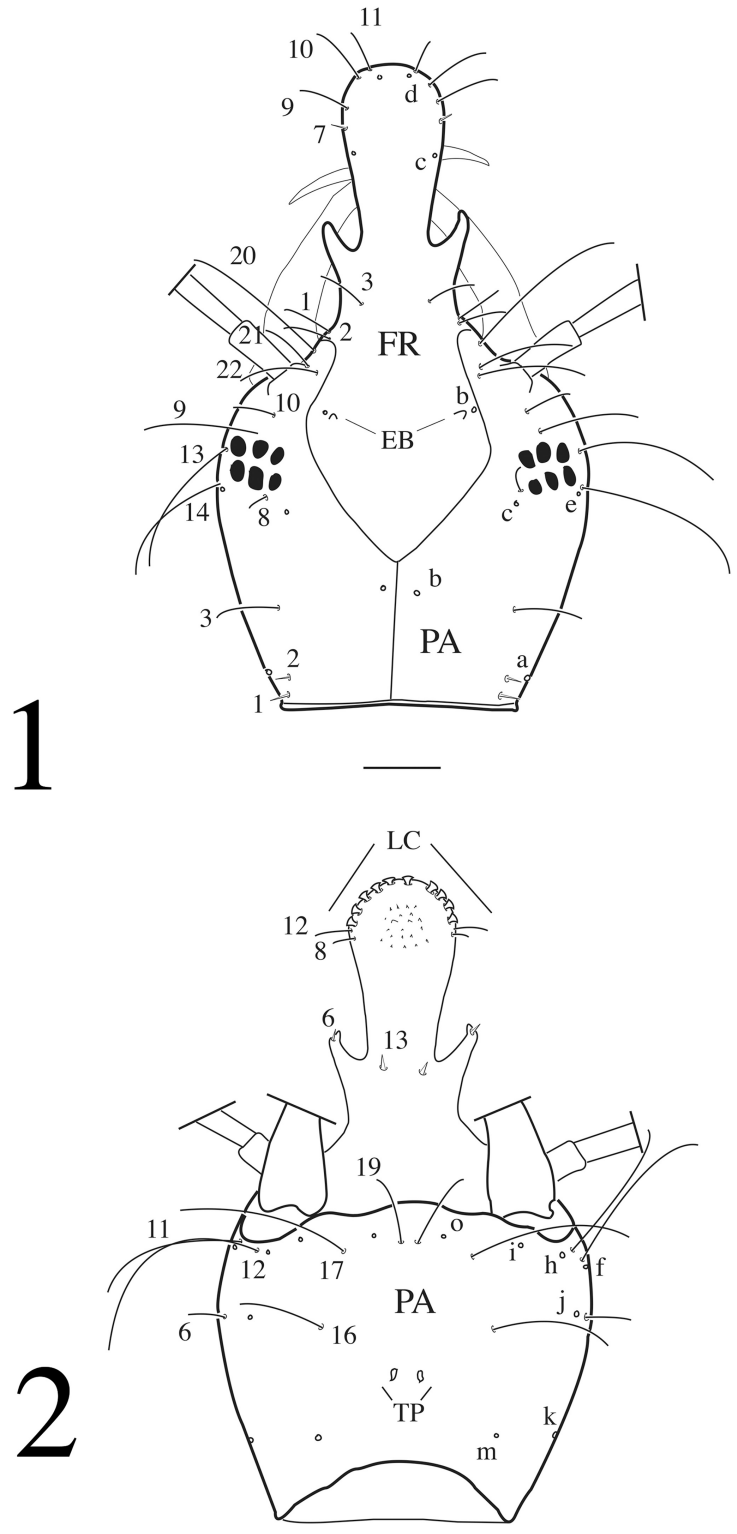

Figs. 1–2. *Megaporus hamatus*, instar I, cephalic capsule. **1)** Dorsal aspect; **2)** Ventral aspect. EB = egg bursters; FR = frontoclypeus; LC = lamellae clypeales; PA = parietale; TP = tentorial pits. Numbers and lowercase letters refer to primary setae and pores, respectively. Color pattern not represented. Scale bar = 0.1 mm.

Table 1. Measurements and ratios for the larvae of *Megaporus hamatus* (MHAM) and *M. gardnerii* (MGAR); l = length; w = width; ** = missing data.

	MHAM			MGAR
Measure	**Instar I (*n* = 2)**	**Instar II (*n* = 5)**	**Instar III (*n* = 5)**	**Instar III (*n* = 2)**
HL (mm)	0.82–0.85	1.28–1.33	1.95–2.13	2.31–2.35
HW (mm)	0.48–0.51	0.80–0.85	1.40–1.48	1.65
FRL (mm)	0.63–0.66	0.97–1.03	1.48–1.60	1.75–1.81
OCW (mm)	0.31–0.33	0.50–0.54	0.94-1.00	1.05–1.08
HL/HW	1.69–1.73	1.53–1.60	1.39–1.45	1.40–1.42
HL/LAS	2.55–2.69	1.42–1.53	1.01–1.08	1.06–1.08
HW/OCW	1.54	1.57–1.62	1.40–1.64	1.54–1.57
A/HW	1.21–1.23	0.98–1.03	0.72–0.78	0.68–0.72
A3/A2	1.30–1.41	1.11–1.24	0.96–1.00	1.00–1.05
A4/A3	0.28–0.37	0.24–0.28	0.22–0.26	0.24–0.25
A3'/A4	0.46–0.71	0.59–0.71	0.69–0.79	0.75
MNL/MNW	4.67–4.84	4.13–4.58	4.31–4.83	4.68–5.04
MNL/HL	0.50	0.51–0.52	0.49–0.52	0.50–0.53
A/MP	1.27–1.30	1.14–1.17	1.01–1.10	**
MP2/MP1	1.15–1.20	0.98–1.03	0.75–0.80	**
MP/LP	1.12–1.19	1.18–1.26	1.12–1.25	**
LP2/LP1	1.31–1.37	0.98–1.12	0.76–0.89	0.81–0.82
L1 (mm)	1.46–1.52	2.17–2.28	3.09–3.29	3.53–3.56
L2 (mm)	1.65–1.75	2.51–2.65	3.58–3.83	4.08–4.09
L3 (mm)	1.84–1.97	2.89–3.02	4.23–4.49	4.81–4.82
L3/L1	1.26–1.30	1.32–1.34	1.35–1.39	1.35–1.36
L3/HW	3.87–3.90	3.42–3.60	3.02–3.10	2.90–2.92
L3(CO/FE)	0.98–0.99	0.97–1.01	1.02–1.05	1.02–1.04
L3(TI/FE)	0.74–0.75	0.71–0.75	0.70–0.73	0.71–0.72
L3(TA/FE)	0.91–0.94	0.78–0.83	0.64–0.69	0.64–0.66
L3(C/TA)	0.48–0.50	0.40–0.44	0.38–0.42	0.36–0.38
LAS (mm)	0.31–0.32	0.87–0.90	1.93–2.03	2.15–2.23
LAS/HW	0.63–0.68	1.04–1.12	1.33–1.40	1.30–1.35
U1 (mm)	1.02–1.28	1.75–1.93	2.28–2.80	2.68–2.98
U1+U2'(mm)	1.33–1.66	2.27–2.41	2.86–3.17	3.26–3.43
U1+U2 (mm)	1.75	2.31–2.46	**	**
U1/U2'	3.20–3.31	3.40–4.43	3.58–5.26	4.58–6.54
U2'/U2	0.82	0.90–0.94	**	**
U1/LAS	3.15–4.03	1.99–2.20	1.18–1.38	1.20–1.38
U1/HW	2.14–2.53	2.08–2.35	1.63–1.93	1.62–1.80
U1+U2'/LAS	4.14–5.25	2.57–2.75	1.49–1.65	1.47–1.60
U1+U2'/HW	2.80–3.29	2.69–2.95	2.04–2.19	1.98–2.08
U1+U2/LAS	5.51	2.62–2.79	**	**
U1+U2/HW	3.46	2.75–3.01	**	**

Hydroporini that have been well studied (i.e. *Antiporus*, *Paroster*, *Barretthydrus,* and *Chostonectes*) by the following combination of characters: HL > 2.00 mm; HL/HW > 1.40; nasale elongate, narrow, spatulate apically (Figs. 1, 15); parietals constricted at level of occipital suture (Fig. 15); labial palpus composed of two palpomeres (Figs. 8–9); prementum lacking spinulae along lateral margins (Figs. 8–9); L3/HW < 3.60; primary seta FE7 present (Fig. 10); natatory setae present on dorsal margin of femora, tibiae and tarsi (Fig. 17); spinulae strongly developed along ventral margin of tibiae and tarsi (Fig. 16); secondary ventral femoral setae compound (Figs. 16–17); siphon very elongate (Fig. 18); urogomphi predominantly with elongate and hair-like secondary setae (Fig. 19); U1/U2' > 3.60; U1/HW > 2.00.

Instar I
(Figs. 1–14)

Description. Body: Subcylindrical, narrowing towards abdominal apex. Measurements and ratios that characterize the body shape are shown in Table 1. **Head:** Head capsule (Figs. 1–2) pear-shaped, tapering posteriorly, not constricted at level of occipital suture; ecdysial suture well-developed, coronal suture short; frontoclypeus

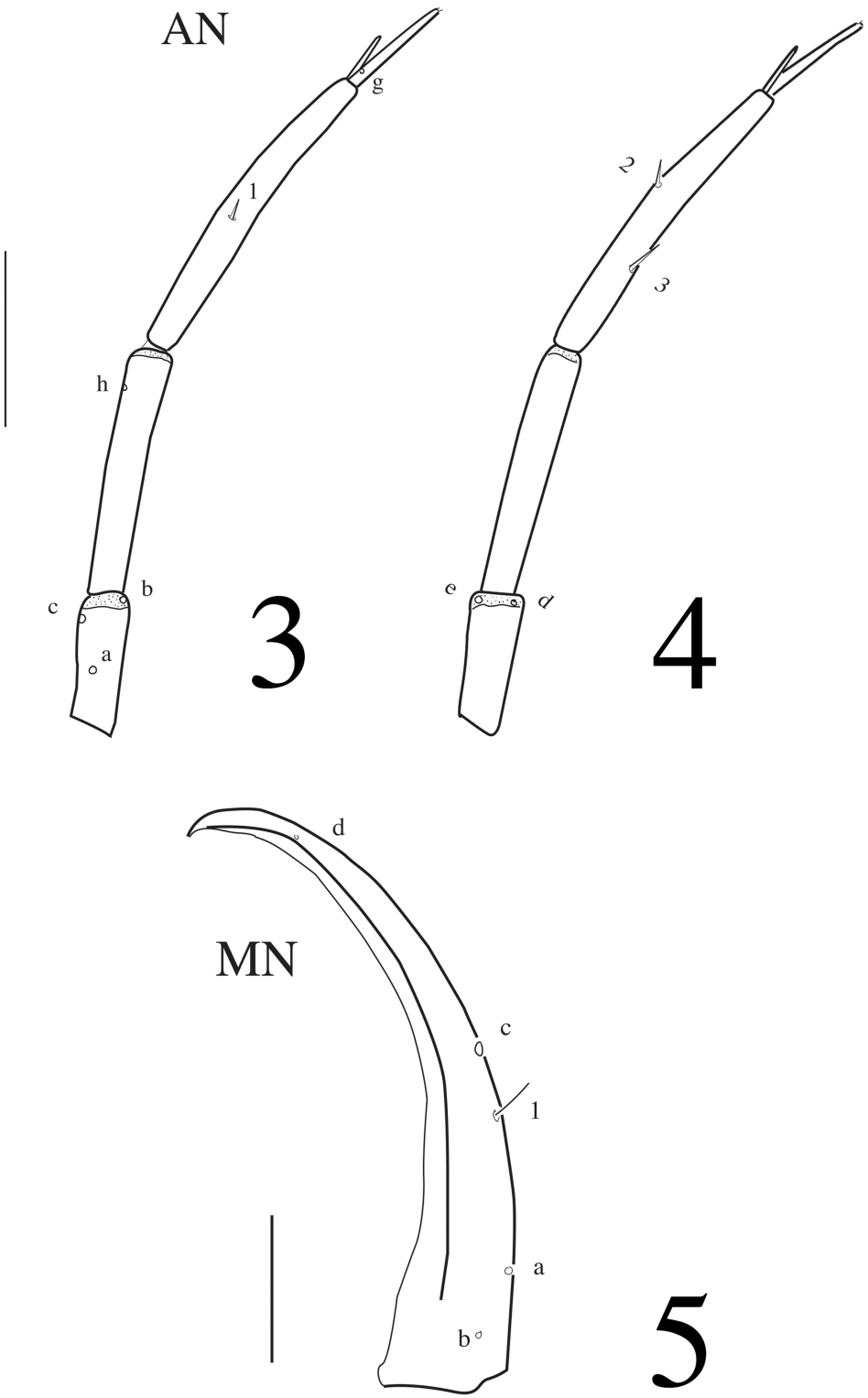

Figs. 3–5. *Megaporus hamatus*, instar I, head appendages. **3)** Antenna, dorsal aspect; **4)** Antenna, ventral aspect; **5)** Mandible, dorsal aspect. AN, antenna; MN, mandible. Numbers and lowercase letters refer to primary setae and pores, respectively. Scale bar = 0.1 mm.

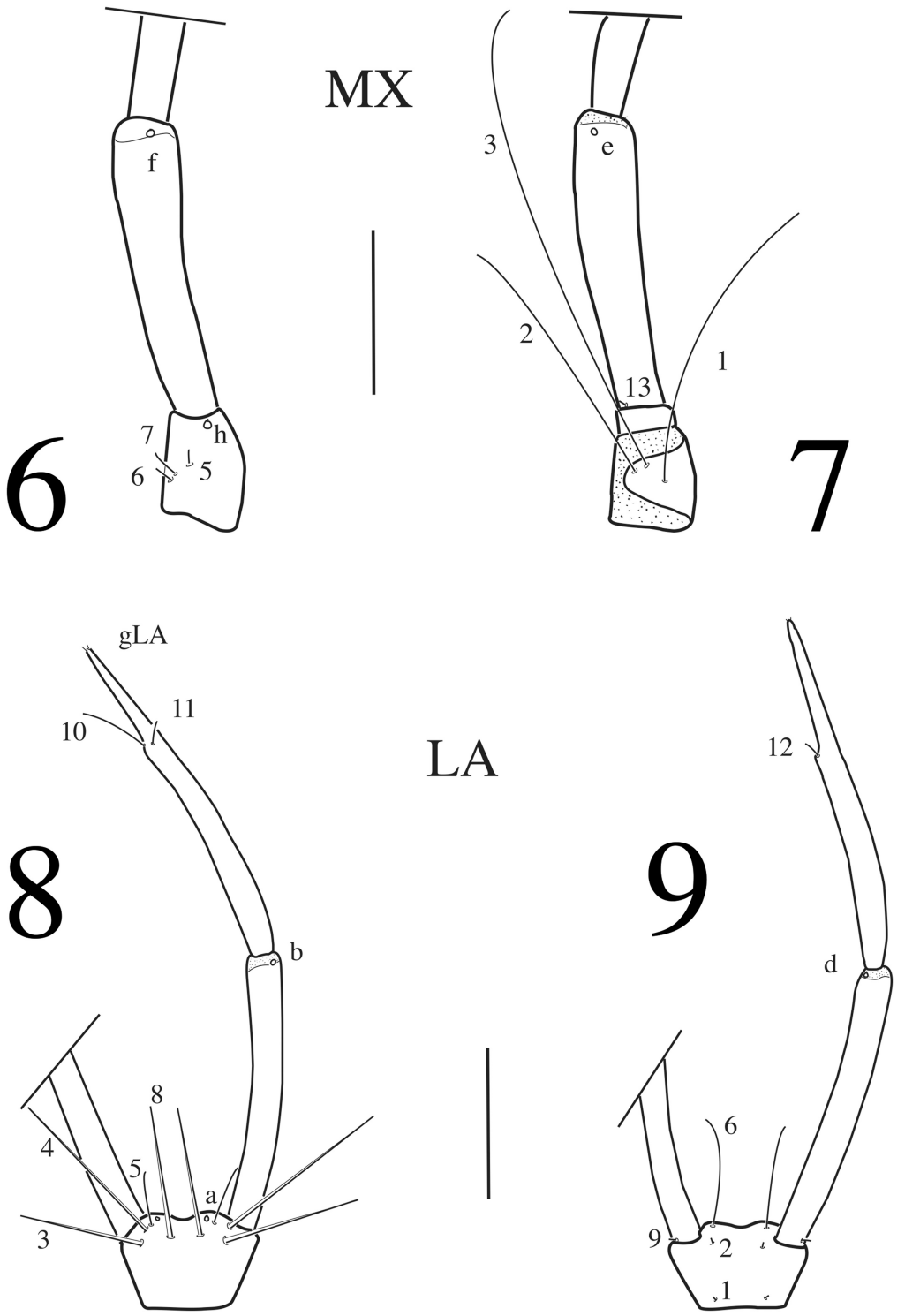

Figs. 6–9. *Megaporus hamatus*, instar I, head appendages. **6)** Proximal portion of maxilla, dorsal aspect; **7)** Proximal portion of maxilla, ventral aspect; **8)** Labium, dorsal aspect; **9)** Labium, ventral aspect; LA, labium; MX, maxilla. Numbers and lowercase letters refer to primary setae and pores, respectively. Scale bars = 0.1 mm.

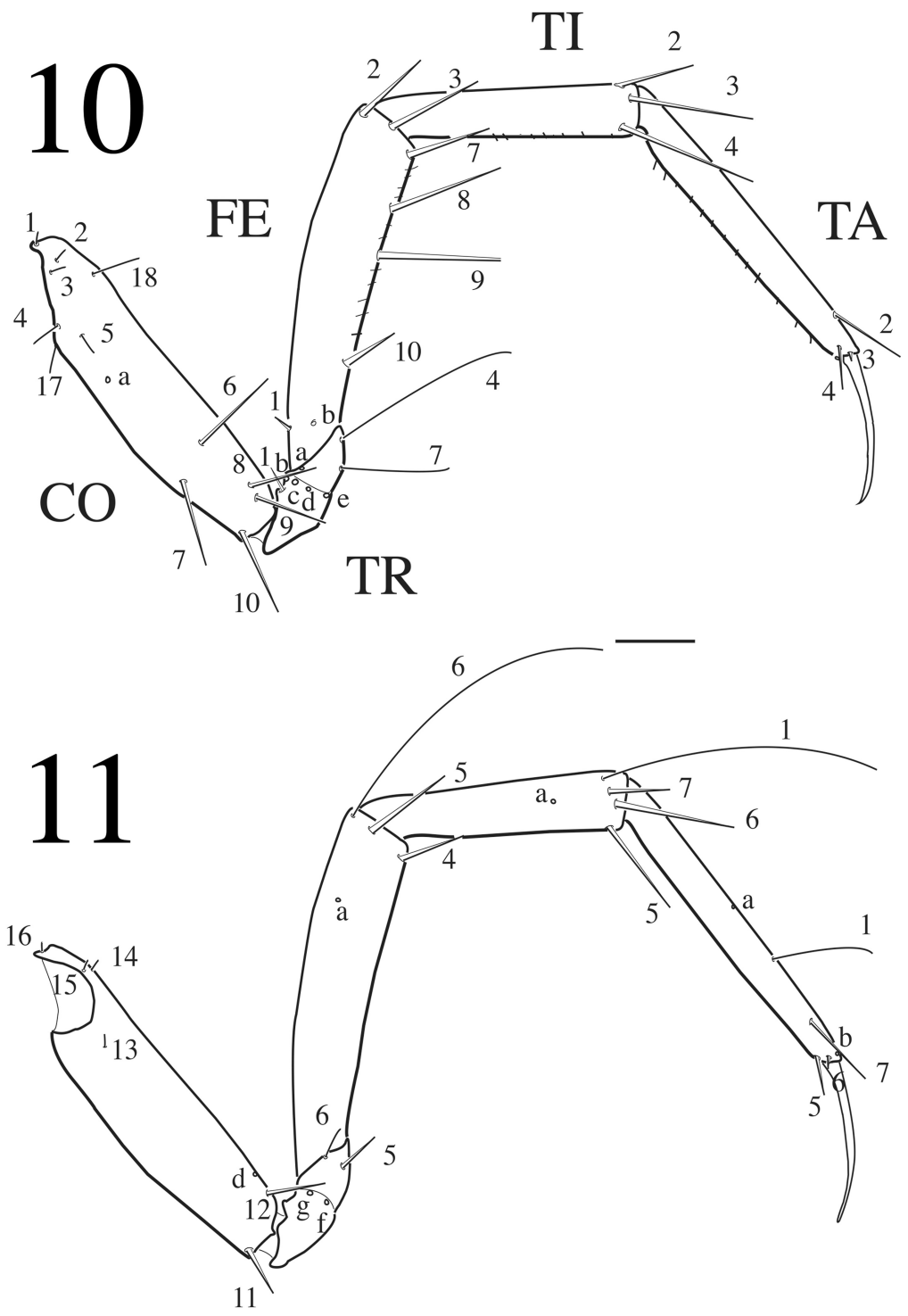

Figs. 10–11. *Megaporus hamatus*, instar I, metathoracic legs. **10)** Anterior surface; **11)** Posterior surface. CO, coxa; FE, femur; TA, tarsus; TI, tibia; TR, trochanter. Numbers and lowercase letters refer to primary setae and pores, respectively. Scale bar = 0.1 mm.

elongate, bluntly rounded, and spatulate apically, with well-developed lateral branches, anteroventral margin with 10 ventral lamellae clypeales (Bertrand 1972); dorsal surface with two spine-like egg bursters (ruptor ovi of Bertrand 1972) at about mid-length; ocularium present, six stemmata not visible ventrally and subdivided into two vertical series; epicranial plates meeting ventrally; tentorial pits

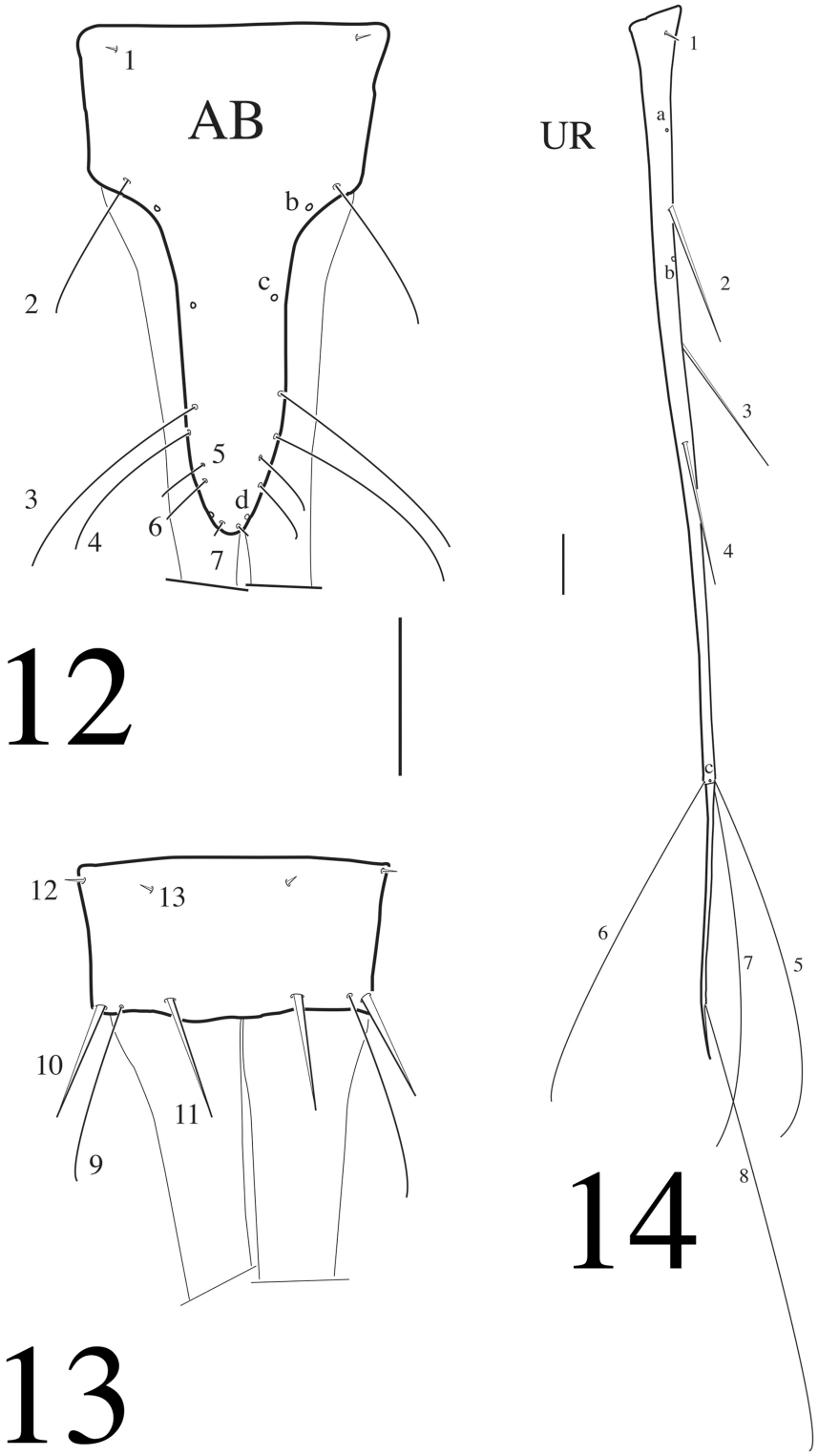

Figs. 12–14. *Megaporus hamatus*, instar I. **12)** Abdominal segment VIII, dorsal aspect; **13)** Abdominal segment VIII, ventral aspect; **14)** Urogomphus, dorsal aspect. AB, abdominal segment VIII; UR, urogomphus. Numbers and lowercase letters refer to primary setae and pores, respectively. Scale bars = 0.1 mm.

Table 2. Measurements and ratios for instar III of selected genera of Sternopriscina: *Antiporus* (ANTI), *Barretthydrus* (BARR), *Chostonectes* (CHOS), *Megaporus* (MEGA), epigaeic *Paroster* (PARE), hypogaeic *Paroster* (PARH). *n* = number of species.

Measure	ANTI[1] (*n* = 7)	BARR[2] (*n* = 2)	CHOS[3] (*n* = 2)	MEGA (*n* = 2)	PARE[4] (*n* = 6)	PARH[4] (*n* = 7)
HL (mm)	1.43–2.12	1.24–1.36	1.58–2.00	1.95–2.35	0.69–0.93	0.52–2.23
HW (mm)	0.73–1.20	0.94–1.02	1.00–1.38	1.40–1.65	0.55–0.75	0.32–1.43
FRL (mm)	1.08–1.65	0.97–1.05	1.24–1.63	1.48–1.81	0.55–0.75	0.39–1.68
OCW (mm)	0.54–0.64	0.56–0.65	0.55–0.93	0.94–1.08	0.45–0.60	0.22–0.60
HL/HW	1.60–2.00	1.24–1.35	1.45–1.60	1.39–1.45	1.18–1.43	1.45–1.85
HL/LAS	3.40–5.30	3.91–4.66	1.63–2.49	1.01–1.08	2.05–2.45	3.17–7.25
HW/OCW	1.40–1.67	1.57–1.70	1.49–1.90	1.40–1.64	1.09–1.33	1.37–4.60
A/HW	0.90–1.36	0.70–0.77	0.87–1.05	0.68–0.78	0.50–0.67	0.65–0.82
A3/A2	0.86–1.16	0.84–1.00	0.91–1.09	0.96–1.05	0.87–1.22	0.82–1.54
A4/A3	0.16–0.22	0.30–0.38	0.17–0.20	0.22–0.26	0.39–0.51	0.20–0.57
A3'/A4	0.60–0.96	0.76–0.98	0.61–0.81	0.69–0.79	0.66–0.91	0.70–1.00
MNL/MNW	4.24–5.99	3.74–4.74	4.03–4.69	4.31–5.04	3.32–4.40	3.95–5.52
A/MP	1.00–1.20	1.00–1.07	0.81–1.14	1.01–1.10	0.82–1.09	0.84–1.11
MP2/MP1	0.74–1.01	0.86–1.00	0.85–0.88	0.75–0.80	0.82–1.24	0.71–1.10
MP/LP	1.31–1.79	1.16–1.25	1.32–1.59	1.12–1.25	1.16–1.45	1.29–1.71
LP2/LP1	0.74–1.09	0.81–0.95	0.76–0.93	0.76–0.89	0.81–1.10	0.67–1.29
L1 (mm)	2.33–3.48	2.03–2.19	2.75–3.72	3.09–3.56	1.16–1.58	0.71–2.96
L3 (mm)	3.05–4.92	2.80–3.09	3.78–5.08	4.23–4.82	1.52–2.25	0.87–3.13
L3/L1	1.28–1.40	1.36–1.42	1.36–1.41	1.35–1.39	1.25–1.50	1.05–1.22
L3/HW	3.83–4.40	2.96–3.15	3.60–3.86	2.90–3.10	2.41–3.52	2.16–2.67
LAS (mm)	0.31–0.54	0.28–0.34	0.65–1.23	1.93–2.23	0.34–0.43	0.15–0.50
LAS/HW	0.36–0.56	0.28–0.35	0.62–1.00	1.30–1.40	0.49–0.68	0.14–0.49
U1 (mm)	2.34–3.65	1.29–1.69	2.09–3.08	2.28–2.98	1.12–2.30	0.75–2.73
U1+U2' (mm)	2.89–4.43	1.99–2.19	2.61–3.80	2.86–3.43	1.62–2.26	0.95–3.12
U1/U2'	3.98–6.54	2.87–3.33	3.62–4.44	3.58–6.54	4.00–6.46	3.29–7.90
U1/LAS	5.24–9.39	4.56–6.08	2.43–3.53	1.18–1.38	3.14–6.28	4.50–7.38
U1/HW	2.59–3.59	1.37–1.67	1.99–2.32	1.98–2.19	1.80–4.00	1.77–2.70

[1] Alarie and Watts (2004); [2] Alarie *et al*. (2018); [3] Alarie *et al*. (2019); [4] Alarie *et al*. (2009).

visible medio-ventrally at about mid-length. Antenna (Figs. 3–4) elongate, distinctly longer than HW; composed of four antennomeres, A2 and A3 longest, A1 shortest; A3' relatively elongate, shorter than A4; A3 lacking a ventroapical spinula. Mandible (Fig. 5) prominent, falciform, distal half projected inwards and upwards, apex sharp; mandibular channel present. Maxilla (Figs. 6–7) with stipes short and thick, incompletely sclerotized ventrally; cardo fused to stipes; galea and lacinia absent; MP elongate, distinctly shorter than antenna, composed of three palpomeres; MP2 longest, MP3 shortest. Labium (Figs. 8–9) with prementum subtrapezoidal, about as long as broad, lacking lateral marginal spinulae; LP elongate, distinctly shorter than MP, composed of two palpomeres; LP2 subfusiform, distinctly longer than LP1. **Thorax:** Terga convex, pronotum slightly shorter than meso- and metanota combined, meso- and metanota subequal; protergite subrectangular to subovate, more developed than meso- and metatergites; anterotransverse carina present on meso- and metatergum; thoracic sterna membranous; spiracles absent. **Legs:** Long (Figs. 10–11), composed of six articles (*sensu* Lawrence 1991); L1 shortest, L3 longest; CO narrow, elongate, TR divided into two parts by an annulus, FE, TI, and TA slender, subcylindrical, PT with two long, slender, slightly curved claws; posterior claw shorter than anterior claw on L1 and L2, posterior claw longer than anterior claw on L3; tibiae and tarsi with spinulae along ventral margin; marginal spinulae faint to almost lacking on metathoracic leg. **Abdomen:** Eight-segmented (Figs. 12–13); segments I–VI sclerotized dorsally, membranous ventrally; segment VII sclerotized both dorsally and ventrally, ventral sclerite independent from dorsal one; tergites I–VII narrow, transverse, rounded laterally, lacking sagittal line and anterotransverse carina; segment VIII (= LAS) the longest, completely sclerotized, ring-like, strongly constricted at point of insertion of urogomphus, distinctly shorter than HW; projected backwards into an elongate siphon; spiracles absent lateroventrally on segments I–VII. **Urogomphus:** Very long (Fig. 14), composed of two urogomphomeres; U1 much longer than segment VIII; U2 much shorter than U1. **Chaetotaxy:** Similar to that of generalized Hydroporinae larva (Alarie 1991;

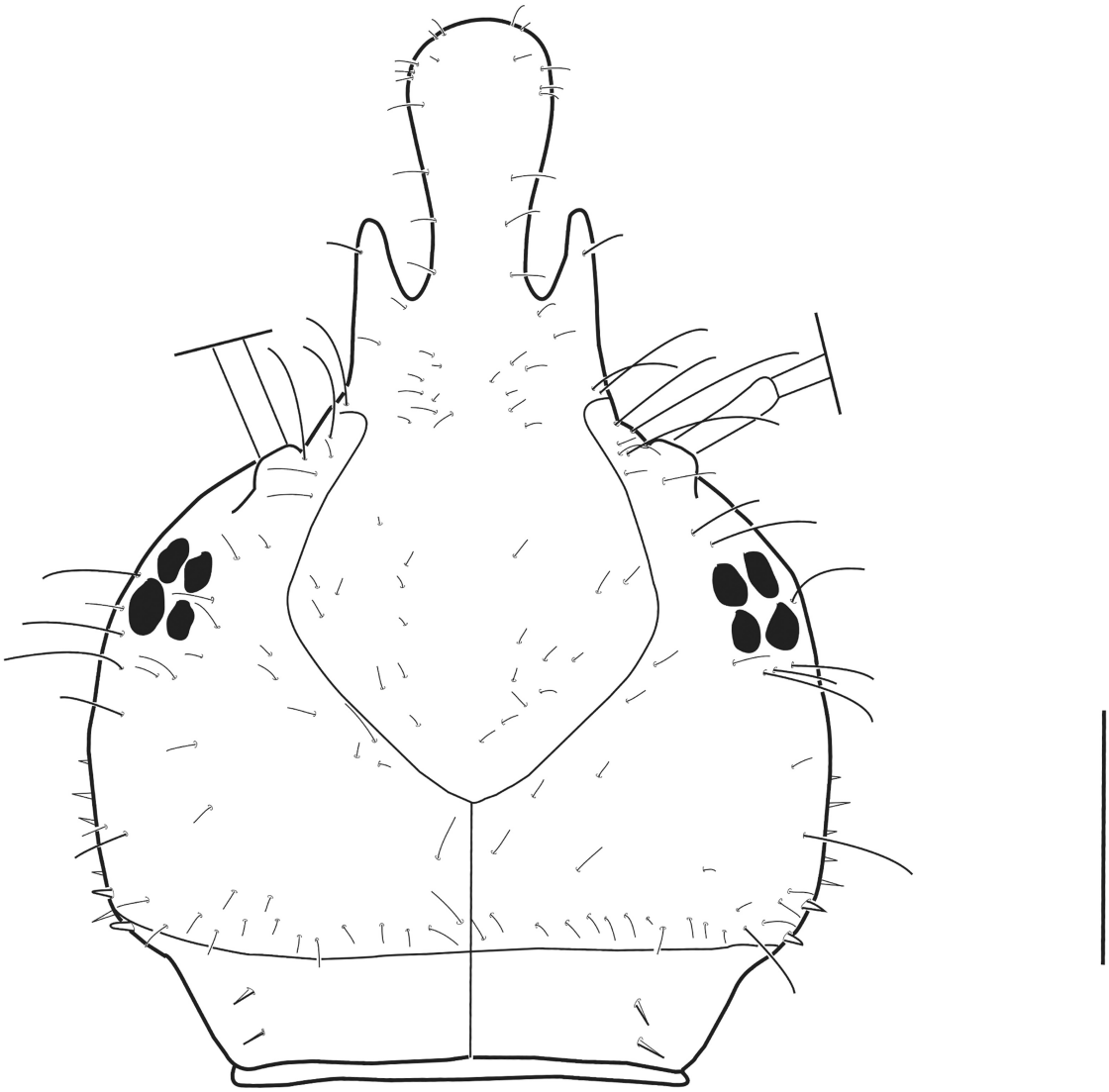

Fig. 15. Dorsal view of cephalic capsule of *Megaporus hamatus*, instar III. Color pattern not represented. Scale bar = 0.5 mm.

Alarie and Harper 1990; Alarie and Michat 2007a; Alarie *et al.* 1990) except for the following features (Figs. 1–14): pores PAd and ANf absent; pore ANh distal; setae MX4 and TR2 absent; pore FEa articulated distally, close to seta FE5; seta FE6 elongate and hair-like; seta TI7 short, spine-like; setae AB2 and AB3 not articulated at about same level; seta AB10 spine-like; seta UR2 and UR3 not contiguously articulated, seta UR4 articulated posteriorly; setae UR5, UR6 and UR7 elongate and hair-like; seta UR8 inserted subapically.

Instar II

Description. As instar I except as follows: **Body:** Measurements and ratios that characterize the body shape are shown in Table 1. **Head:** Frontoclypeus with anteroventral margin with 18–22 ventral lamellae clypeales, egg bursters lacking; parietale constricted at level of occipital carina. Maxilla, MP1 subequal to MP2 in length. Labium, LP2 subequal to slightly longer than LP1. **Thorax:** Protergum with an anterotransverse carina. **Legs:** Position and number of secondary setae in Table 3; natatory setae present on dorsal margin of femora, tibiae, and tarsi; elongate ventral and spine-like spinulae present on all tibiae and tarsi. **Abdomen:** Segment VII completely sclerotized, ring-like, all tergites with an anterotransverse carina; LAS subequal to sligthly longer than HW. **Chaetotaxy:** Head capsule with numerous secondary setae; lateroventral margin of PA with 5–7 spine-like setae; AN, MX, and LA lacking secondary setae; MN with 1

Table 3. Number of secondary setae on the legs of *Megaporus hamatus* (MHAM) and *M. gardnerii* (MGAR). CO = coxa; FE = femur; TA = tarsus; TI = tibia; TR = trochanter; total is the total number of secondary setae on segment; A = anterior; AD = anterodorsal; Di = distal; AV = anteroventral; D = dorsal; NS = natatory setae; PD = posterodorsal; Pr = proximal; PV = posteroventral; V = ventral; *n* = number of specimens studied.

		MHAM		MGAR
Segment	**Sensillar series**	**Instar II (*n* = 4)**	**Instar III (*n* = 5)**	**Instar III (*n* = 2)**
ProCO	D	4–5	7–8	9–11
	A	1–2	4–5	6–8
	V	2–5	5–12	8–11
	Total	7–11	17–24	25–28
ProTR	Pr	1	2–3	2
	Di	0–1	0	1
	Total	1–2	2–3	3
ProFE	NS (PD)	6–7	14–18	20–22
	AD	4–6	7–9	11–14
	AV	16–18	24–29	23–28
	PV	2–4	9–12	12–13
	Total	28–35	58–67	71–72
ProTI	NS(PD)	6–9	20–26	25–27
	AD	2–3	6–8	6–8
	AV	0–2	4–6	3–4
	PV	3–4	2–4	3–4
	Total	13–17	33–41	39–41
ProTA	NS(PD)	5–6	12–15	19–20
	AD	2–3	2–5	4
	AV	1–2	1–2	2–4
	PV	3–4	3–5	5
	Total	11–15	21–24	31–32
MesoCO	D	4–5	7–9	13–14
	A	0–2	3–5	8–12
	V	2–4	8–13	7–8
	Total	8–10	19–25	29–33
MesoTR	Pr	1–2	3	3–5
	Di	1	0–1	1
	Total	2–3	3–4	4–6
MesoFE	NS(PD)	5–7	15–20	21–23
	AD	7–8	11–13	19
	AV	12–19	26–31	21–22
	PV	10–15	24–29	22
	Total	35–49	78–93	83–84
MesoTI	NS (PD)	9–10	20–26	31–32
	AD	5–7	6–8	10–13
	AV	3–5	4–6	5–6
	PV	2–3	2–4	3–6
	Total	20–25	33–41	49–57
MesoTA	NS(PD)	6–9	16–23	28–29
	AD	3–5	4–6	5–6
	AV	3–5	4–5	6
	PV	3–4	2–6	5–6
	Total	18–21	28–35	45–46
MetaCO	D	4–6	8–10	12–13
	A	0	4–7	11
	V	2–4	7–14	12–13
	Total	7–9	22–28	35–37
MetaTR	Pr	1–2	4	4–5
	Di	1–2	1–2	1
	Total	2–3	5–6	5–6
MetaFE	NS (PD)	4–6	14–21	20–23
	AD	9–11	15–18	26–30

Continued on next page

Table 3. Continued.

		MHAM		MGAR
Segment	**Sensillar series**	**Instar II (*n* = 4)**	**Instar III (*n* = 5)**	**Instar III (*n* = 2)**
	AV	10–16	25–31	24–25
	PV	13–19	30–32	23–26
	Total	36–52	88–101	97–100
MetaTI	NS(PD)	8–12	24–29	30–32
	AD	6–8	10–12	14–15
	AV	6–8	8–10	5–9
	PV	3	4–6	4–6
	Total	23–31	47–54	55–60
MetaTA	NS(PD)	8–10	18–27	29–31
	AD	5–6	6–8	9
	AV	5–7	6–7	7–9
	PV	3–5	3–5	6
	Total	24–28	36–44	53

hair-like secondary seta on basoexternal margin; thoracic and abdominal sclerites I–VIII with numerous secondary setae mainly on posterior half; natatory setae present on dorsal margin of femora, tibiae, and tarsi (as in Fig. 17); secondary leg setation detailed in Tables 3; U with predominantly elongate and hair-like secondary setae (as in Fig. 19).

Instar III
(Figs. 15–19)

Description: As instar II except as follows: **Body:** Measurements and ratios that characterize the body shape are shown in Tables 1–2. **Head:** Frontoclypeus with anteroventral margin with 25–31 ventral lamellae clypeales (Fig. 15). Antenna shorter than HW, A3 subequal to A2 in length. Maxilla with MP1 longer than MP2; Labium with LP2 shorter than LP1. **Thorax:** Meso- and metathoracic terga with an anterotransverse carina; sagittal line visible; mesopleural region with a spiracular opening on each side. **Legs:** Position and number of secondary setae shown in Table 3 (Figs. 16–17). **Abdomen:** Mesopleural region of segments I–VII with a spiracular opening on each side (Figs. 18–19). **Chaetotaxy:** Head capsule with numerous secondary setae; lateroventral margin of PA with 13–15 secondary spine-like setae (Fig. 15); secondary leg setation detailed in Tables 3–4 and Figs. 16–17.

Megaporus hamatus (Clark, 1862)
(Figs. 1–19)

Source of Material. Larvae were collected with adults at the following localities: **South Australia,** 10 km N of Coonawarra, 19.X.1999, C. H. S. Watts, leg.; 2 km South of Penola, 19.X.1999, C. H. S. Watts leg.

Diagnostic Combination (Instar III). The third instar of *Megaporus hamatus* can easily be distinguished from that of the closely similar *M. gardnerii* by its smaller size (HL < 2.10 compared to > 2.30) and a lesser number of D secondary setae on coxae and natatory setae on femora, tibiae and tarsi (Table 3).

Instar I
(Figs. 1–14)

Description. Color. Not provided owing to the bad state of preservation of the only specimen available. **Body:** Measurements and ratios that characterize the body shape are shown in Table 1. **Head:** Head capsule (Figs. 1–2) with HL = 0.80–0.85 mm; HL/LAS = 2.55–2.69. **Abdomen:** LAS = 0.31–0.32 mm; LAS/HW = 0.63–0.68; U1 = 1.02–1.28 mm; U1/LAS = 3.15–4.03 (Figs. 12–14).

Instar II

Description: As instar I except as follows: **Body:** Measurements and ratios that characterize the body shape are shown in Table 1. **Head:** Head capsule with HL = 1.28–1.33 mm; HL/LAS = 1.53–1.60. **Abdomen:** LAS = 1.04–1.12 mm; LAS/HW = 1.04–1.12; U1 = 1.75–1.93 mm; U1/LAS = 1.99–2.20. **Chaetotaxy:** Secondary leg setation detailed in Table 3.

Instar III
(Figs. 15–19)

Description: As instar II except as follows: **Color:** Head capsule dark yellow to pale brown, with several pale yellow maculae posteriorly over

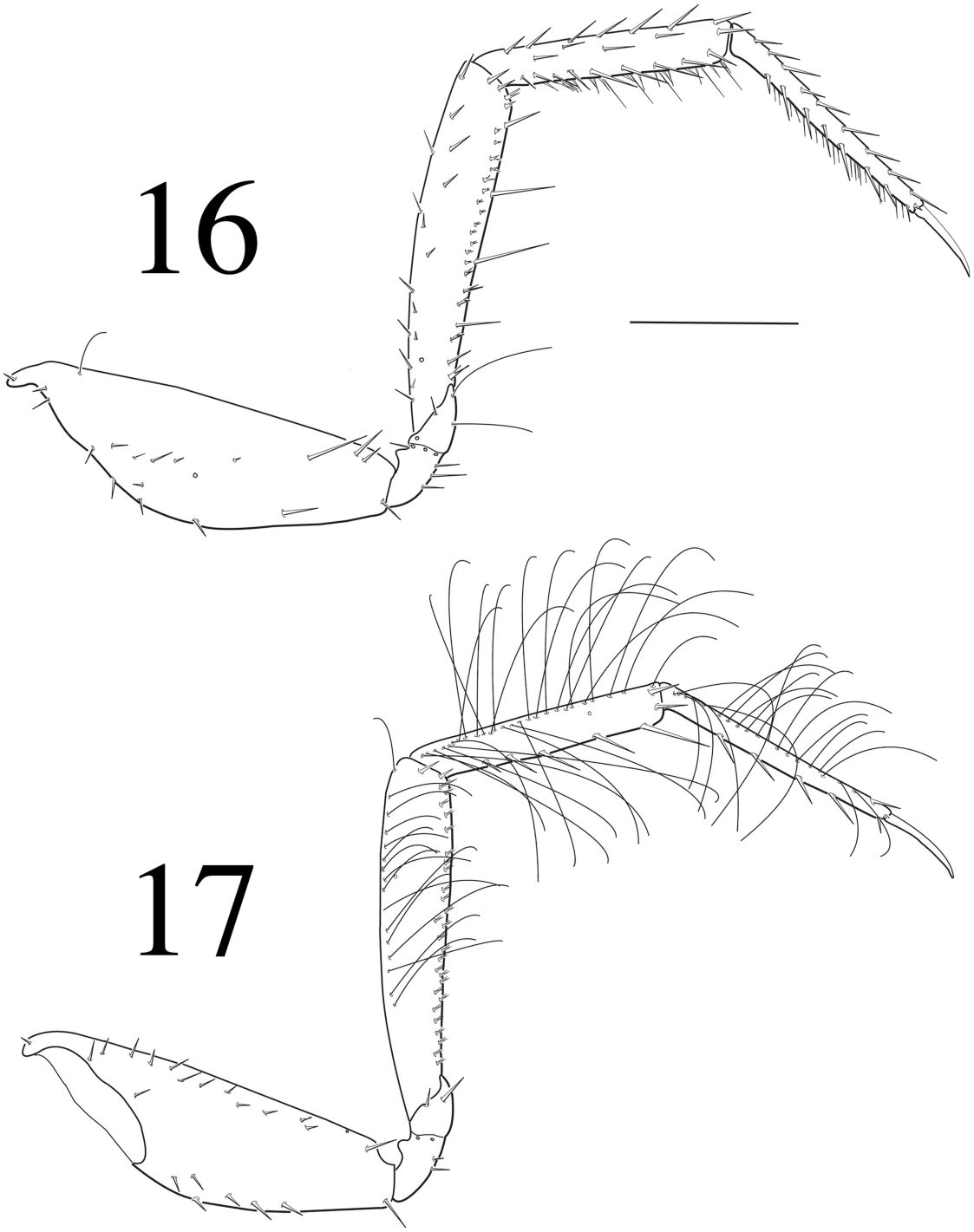

Figs. 16–17. Metathoracic leg of *Megaporus hamatus*, instar III. **16)** Anterior surface; **17)** Posterior surface. Scale bar = 0.5 mm.

frontoclypeus and parietale; head appendages yellow, A4 infuscate; mandible yellow to pale brown proximally, dark brown distally; thoracic terga yellow laterally, brownish mesally; legs predominantly yellow except coxae, brown over proximal 2/3; abdominal terga predominantly brown, segments 1–6 paler along lateral margin; siphon much darker apically; urogomphomere 1 yellow proximally, blackish over distal half; urogomphomere 2 yellow. **Body:** Measurements and ratios that characterize

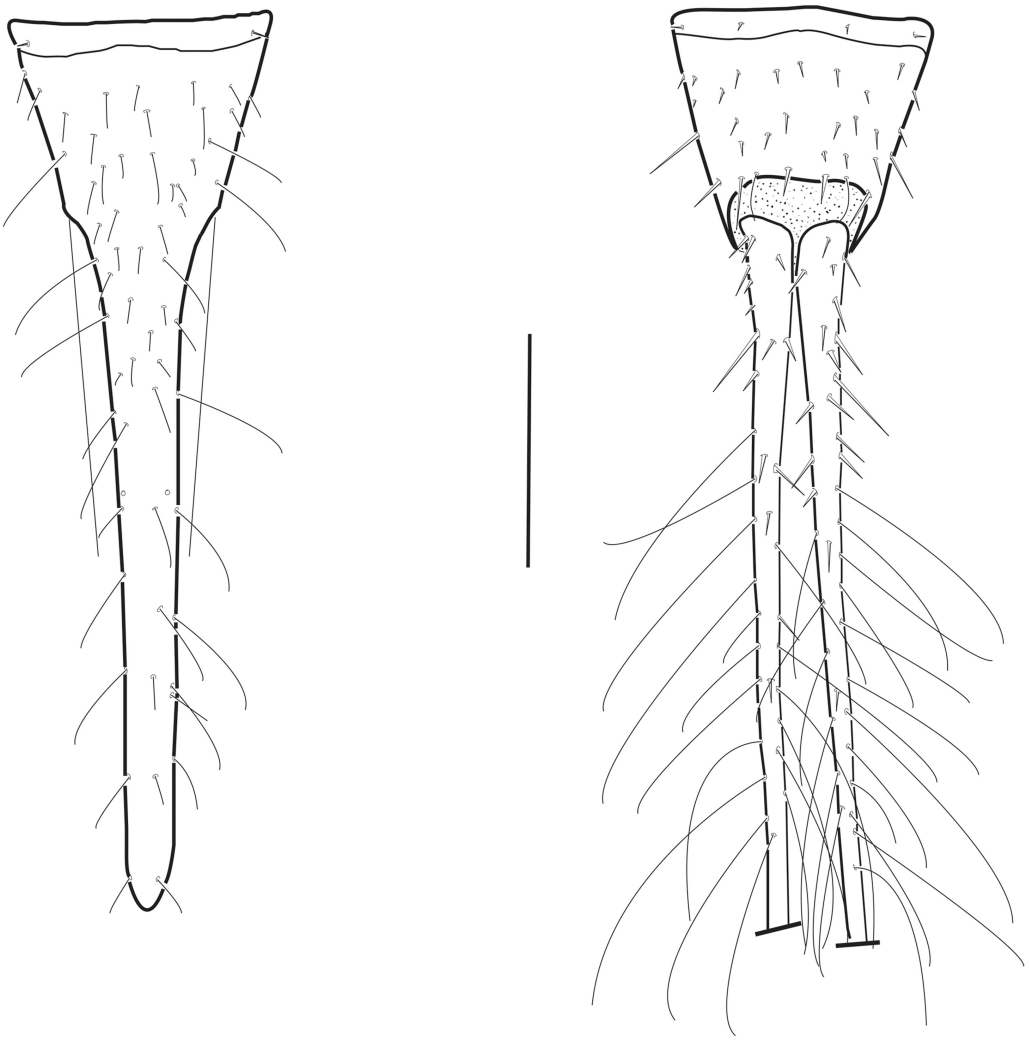

18 19

Figs. 18–19. Last abdominal segment and urogomphi of *Megaporus hamatus*, instar III. **18)** Dorsal surface; **19)** Ventral surface. Scale bar = 0.5 mm.

the body shape shown in Table 1. **Head:** Head capsule (Fig. 15) with HL = 1.95–2.13 mm; HL/LAS = 1.01–1.08. **Abdomen:** LAS = 1.93–2.03 mm; LAS/HW = 1.33–1.40; U1 = 2.28–2.80 mm; U1/LAS = 1.18–1.38 (Figs. 18–19). **Chaetotaxy:** Secondary leg setation detailed in Table 3 and Figs. 16–17.

Megaporus gardnerii (Clark, 1862)

Source of Material. Larvae were collected in association with adults at the following locality: **South Australia,** Mandina Marshes South East, 15.X.2000, C. H. S. Watts leg.

Diagnostic Combination (Instar III). See under *Megaporus hamatus*.

Instar I

No specimen available for study.

Instar II

No specimen available for study.

Table 4. Number of secondary setae on the legs of third instars of selected genera of Australian Hydroporini (Sternopriscina): *Antiporus* Sharp (ANTI), *Barretthydrus* Lea (BARR); *Chostonectes* Sharp (CHOS); *Megaporus* Brinck (MEGA); *Paroster* Sharp (PARO); CO = coxa; FE = femur; TA = tarsus; TI = tibia; TR = trochanter; total is the total number of secondary setae on segment. Sensillar series: A = anterior; AD = anterodorsal; Di = distal; AV = anteroventral; D = dorsal; NS = natatory setae; PD = posterodorsal; Pr = proximal; PV = posteroventral; V = ventral; *n* = number of species studied.

Segment	Sensillar series	ANTI (*n* = 7)	BARR (*n* = 2)	PARO (*n* = 9)	CHOS (*n* = 2)	MEGA (*n* = 2)
ProCO	D	5–19	4–8	3–9	4–11	7–11
	A	1–12	2–3	0–3	1–6	4–8
	V	3–19	5–10	0–4	4–9	5–12
	Total	10–43	11–21	3–14	10–26	17–28
ProTR	Pr	1–6	1	0	1–4	2–3
	Di	0–3	0–2	0	0–2	0–1
	Total	1–8	1–3	0	1–5	2–3
ProFE	NS (PD)	14–28	9–12	0	21–33	14–22
	AD	12–21	6–12	2–11	8–17	7–14
	AV	15–28	13–20	1–13	16–39	23–29
	PD	0–1	0	0–5	0–3	0
	PV	6–16	7–14	2–13	9–17	9–13
	Total	50–84	35–58	10–38	57–106	58–72
ProTI	NS(PD)	14–28	12–17	0	15–36	20–27
	AD	4–13	3–5	0–4	4–9	6–8
	AV	3–10	2–4	0–4	0–4	3–6
	PD	0	0	0–5	0	0
	PV	4–8	2–7	0–5	3–6	2–4
	Total	31–57	19–31	1–18	23–54	33–41
ProTA	NS(PD)	11–27	9–12	0	14–27	12–20
	AD	2–10	2–3	0–3	4–8	2–5
	AV	5–12	0	0–4	0–1	1–4
	PD	0	0	0-4	0	0
	PV	5–9	4–6	0–5	4–7	3–5
	Total	27–56	15–19	1–13	23–42	21–32
MesoCO	D	4–24	6–10	1–9	6–13	7–14
	A	0–14	2–6	0–4	1–8	3–12
	V	2–21	5–11	0–6	4–12	7–13
	Total	8–54	15–29	2–17	12–33	19–33
MesoTR	Pr	1–7	1–3	0–2	2–4	3–5
	Di	0–5	1–2	0	0–2	0–1
	Total	1–12	2–5	0–2	2–6	3–6
MesoFE	NS(PD)	13–31	11–16	0	18–34	15–23
	AD	13–24	7–17	3–10	12–26	11–19
	AV	16–26	13–18	5–14	17–38	21–31
	PD	0-2	0	0-8	0-4	0
	PV	10–25	11–19	5–23	13–29	22–29
	Total	56–101	44–64	14–42	65–128	78–93
MesoTI	NS (PD)	17–39	18–22	0	24–46	20–32
	AD	6–19	6–11	1–5	9–17	6–13
	AV	5–17	5–13	1–6	5–11	4–6
	PD	0	0	0-10	0-3	0
	PV	6–16	6–10	1–9	4–7	2–6
	Total	43–83	36–51	3–22	45–80	33–57
MesoTA	NS(PD)	15–40	16–19	0	21–37	16–29
	AD	4–10	3–7	0–2	6–12	4–6
	AV	6–13	4–8	0–7	6–9	4–6
	PD	0	0	0–6	0	0
	PV	6–13	2–7	1–7	5–8	2–6
	Total	37–69	26–37	3–20	39–64	28–46
MetaCO	D	5–30	5–10	2–9	6–13	8–13
	A	0–18	5–9	0–6	3–9	4–11
	V	3–25	4–14	0–8	5–16	7–14
	Total	10–63	14–32	2–23	14–37	22–37
MetaTR	Pr	1–8	2–3	0–3	1–7	4–5

Continued on next page

Table 4. Continued.

Segment	Sensillar series	ANTI (*n* = 7)	BARR (*n* = 2)	PARO (*n* = 9)	CHOS (*n* = 2)	MEGA (*n* = 2)
	Di	0–6	2–3	0	0–5	1–2
	Total	1–13	4–5	0–3	3–12	5–6
MetaFE	NS (PD)	9–29	6–12	0	11–29	14–23
	AD	15–26	10–18	3–11	16–30	15–30
	AV	10–29	14–24	5–14	15–37	24–31
	PD	0–4	0	0–3	0–3	0
	PV	12–31	8–22	5–31	14–29	23–32
	Total	54–105	43–69	14–55	63–127	88–101
MetaTI	NS(PD)	17–41	20–22	0	22–48	24–32
	AD	7–18	8–16	0–11	12–21	10–15
	AV	5–15	6–10	1–6	6–14	5–10
	PD	0	0	0–6	0	0
	PV	7–18	6–11	1–12	5–12	4–6
	Total	46–84	40–55	5–26	47–87	47–60
MetaTA	NS(PD)	17–42	19–22	0	21–42	18–31
	AD	5–14	4–10	0–3	9–14	6–9
	AV	6–14	5-10	1–9	8-12	6–9
	PD	0	0	0–9	0	0
	PV	7–15	3–9	2–8	6–8	3–6
	Total	42–73	31–47	4–26	48–69	36–53

Instar III

Description: Color: Dark brown larva. Head capsule predominantly dark brown, paler apically over frontoclypeus; parietale and frontoclypeus with several dark yellow maculae; head appendages dark yellow to pale brown, mandible dark brown to black over distal half; thoracic and abdominal terga brown; legs pale brown, coxae darker; urogomphi brown, pale proximally. **Body:** Measurements and ratios that characterize the body shape are shown in Table 1. **Head:** HL = 2.31–2.35 mm; HL/LAS = 1.06–1.08. **Abdomen:** LAS = 2.15–2.23 mm; LAS/HW = 1.30–1.35; U1 = 2.68–2.98 mm; U1/LAS = 1.20–1.38. **Chaetotaxy:** Secondary leg setation detailed in Table 3.

Phylogenetic Analysis

Eighty-four characters (75 binary and nine multistate) were coded for larvae of seven species of Sternopriscina and five outgroups. The characters used and their states are listed in Table 5. The analysis of the data matrix (Table 6) with TNT resulted in two most parsimonious cladograms of 144 steps (CI: 0.65; RI: 0.70), which differed slightly in outgroup topology. The strict consensus tree was calculated (Fig. 20), in which *Megaporus* forms a relatively well-supported clade together with *Chostonectes* and *Antiporus*. Character state changes were mapped on one of the most parsimonious trees (Fig. 21).

Discussion

This study is part of a broader research project aiming at studying the larval morphology of Australasian Hydroporini, also known as Sternopriscina (Miller and Bergsten 2016). The larval description of *Megaporus* provided herein brings to five the number of genera of Sternopriscina for which larvae have been described in much detail including chaetotaxy (the others being *Barretthydrus*, *Antiporus*, *Chostonectes,* and *Paroster*: Alarie and Watts 2004; Alarie *et al.* 2009, 2018, 2019). Morphologically, larvae of these genera are characterized by several character states including: i) frontoclypeus with lateral branches (character 02, Fig. 1); ii) absence of the primary pore ANf (character 22, Figs. 3–4); iii) cardo fused to maxillary stipes (character 25, Fig. 7); iv) absence of the primary seta TR2 (character 42, Fig. 10); and v) presence of elongate urogomphi (character 83) with secondary setae (character 82, Fig. 19).

Within the known Sternopriscina, *Megaporus* stands out in a well-supported clade including *Chostonectes* and *Antiporus* (Bremer support = 4, Bootstrap value = 85) (Fig. 20), which is characterized by (Fig. 21): i) a narrow, more or less parallel-sided nasale (character 00, Figs. 1, 15); ii) a spatulate nasale (character 01, Figs. 1, 15); iii) an elongate cephalic capsule (character 03); iv) elongate antenna (character 06); v) seta FR13 inserted proximally, distinctly posterior to seta FR6 (character 08, Fig. 2); presence of strongly developed ventral marginal spinulae on vi) protibiae (character 46) and vii) protarsi (character 48) of instar III

Table 5. Characters used for the phylogenetic analysis and the coding of states using selected genera of Hydroporinae as outgroups.

(00)	Nasale (instars I–III): (0) broad, subtriangular; (1) narrow, more or less parallel sided.
(01)	Apex of nasale (instars I–III): (0) not spatulate; (1) spatulate.
(02)	Lateral branches of nasale (instars I–III): (0) absent; (1) very small, inconspicuous; (2) well developed, short, not bifid apically.
(03)	Head capsule (instar III): (0) HL/HW < 1.40; (1) HL/HW > 1.40.
(04)	Egg bursters (instar I): (0) located submedially on the frontoclypeus, close to frontal suture; (1) located proximally on the frontoclypeus.
(05)	Seta FR2 (instar I): (0) inserted close to frontal suture; (1) inserted far from frontal suture.
(06)	Antenna (instar III): (0) < 0.80 HW; (1) > 0.90 HW.
(07)	Seta FR7 (instar I): (0) hair-like; (1) spine-like.
(08)	Seta FR13 (instar I): (0) absent; (1) inserted distally, at about level of seta FR6 or higher; (2) inserted proximally, distinctly lower than seta FR6.
(09)	Parietals (at level of occipital suture) (instar III): (0) at most slightly constricted; (1) distinctly constricted.
(10)	Occipital suture (instar I): (0) absent; (1) present.
(11)	Occipital suture (instars II–III): (0) absent; (1) present.
(12)	Stemmata (instars I–II): (0) present; (1) absent.
(13)	Seta PA3 (instar I): (0) inserted contiguously to setae PA1 and PA2; (1) inserted far from setae PA1 and PA2.
(14)	Seta PA18 (instar I): (0) present; (1) absent.
(15)	Pore PAd (instar I): (0) present; (1) absent.
(16)	Pore PAe (instar I): (0) present; (1) absent.
(17)	Pore PAj (instar I): (0) present; (1) absent.
(18)	Pore PAo (instar I): (0) present; (1) absent.
(19)	Secondary spine-like setae on lateral margin of parietals (instars II–III): (0) absent; (1) present.
(20)	Secondary spine-like setae on ventral surface of parietals (instars II–III): (0) absent; (1) present.
(21)	Seta AN3 (instar I): (0) inserted distally; (1) inserted submedially.
(22)	Pore ANf (instar I): (0) present; (1) absent.
(23)	Pore ANh (instar I): (0) absent; (1) present.
(24)	Sensillum MN2 (instar I): (0) with the appearance of a pore or minute seta; (1) with the appearance of a short hair-like seta.
(25)	Cardo (instars I–III): (0) not fused to stipes; (1) fused to stipes.
(26)	Second galeomere (instars I–III): (0) poorly developed, thin and very short; (1) absent, at most a minute bulge.
(27)	Seta MX4 (instar I): (0) present; (1) absent.
(28)	Setae MX8 and MX9 (instar I): (0) present; (1) absent.
(29)	Seta MX10 (instar I): (0) present; (1) absent.
(30)	Pore MXh (instar I): (0) inserted on the galea; (1) inserted on the stipes.
(31)	Pore MXk (instar I): (0) absent; (1) present.
(32)	Elongate spinulae on lateral margin of prementum (instar I): (0) absent; (1) present.
(33)	Labial palpus (instars I–III): (0) composed of two palpomeres; (1) composed of three palpomeres.
(34)	Seta LA2 (instar I): (0) present; (1) absent.
(35)	Seta LA3 (instar I): (0) present; (1) absent.
(36)	Seta LA8 (instar I): (0) inserted distally; (1) inserted proximally.
(37)	Seta LA10 (instar I): (0) inserted subapically; (1) inserted submedially; (2) apically.
(38)	Seta LA11 (instar I): (0) inserted subapically; (1) inserted submedially; (2) apically.
(39)	Seta LA12 (instar I): (0) inserted subapically; (1) inserted submedially; (2) apically.
(40)	Setae LA10 and LA12 (instar I): (0) short or very short; (1) long.
(41)	Secondary pores on ventral surface of prementum (instars II–III): (0) absent; (1) present.
(42)	Seta TR2 (instar I): (0) present; (1) absent.
(43)	Pore FEa (instar I): (0) absent; (1) present.
(44)	Natatory posterodorsal setae on femur (instars II–III): (0) absent; (1) present.
(45)	Secondary anterodorsal setae on femur (instars II–III): (0) absent; (1) present.
(46)	Spinulae on ventral surface of protibiae (instar III): (0) absent or few small disperse spinulae that do not form a distinct row; (1) strongly developed, forming a distinct row.
(47)	Spinulae on ventral surface of meso- and metatibiae (instar III): (0) absent or few small disperse spinulae that do not form a distinct row; (1) strongly developed, forming a distinct row.
(48)	Spinulae on ventral surface of protarsi (instar III): (0) absent or few small disperse spinulae that do not form a distinct row; (1) strongly developed, forming a distinct row.
(49)	Spinulae on ventral surface of meso- and metatarsi (instar III): (0) absent or few small disperse spinulae that do not form a distinct row; (1) strongly developed, forming a distinct row.

Continued on next page

Table 5. Continued.

(50)	Secondary femoral setae (instar III): (0) unifid; (1) bifid or multifid.
(51)	Primary seta FE6 (instars I): (0) very short; (1) very elongate.
(52)	Secondary setae on tibia (instars II–III): (0) absent; (1) present.
(53)	Natatory posterodorsal setae on tibia (instars II–III): (0) absent; (1) present.
(54)	Seta TA1 on metatarsus (instar I): (0) inserted distad to pore TAa; (1) inserted submedially, proximad to pore TAa.
(55)	Secondary dorsal setae on protarsus (instar III): (0) absent; (1) present.
(56)	Secondary posteroventral setae on protarsus (instar III): (0) absent; (1) present.
(57)	Secondary posteroventral setae on metatarsus (instar III): (0) absent; (1) present.
(58)	Natatory posterodorsal setae on tarsus (instars II–III): (0) absent; (1) present.
(59)	Basoventral spinulae on claws (instar I): (0) absent; (1) present.
(60)	Abdominal tergites I–VI (instar I): (0) with anterotransverse carina; (1) without anterotransverse carina.
(61)	Ventral surface of abdominal segments II–III (instar III): (0) sclerotized; (1) membranous.
(62)	Ventral surface of abdominal segments IV–V (instar III): (0) sclerotized; (1) membranous.
(63)	Ventral surface of abdominal segment VI (instars I–III): (0) sclerotized; (1) membranous.
(64)	Abdominal segment VII (instar I): (0) sclerotized dorsally and ventrally, with ventral sclerite independent from dorsal sclerite; (1) completely sclerotized, ring-like.
(65)	Abdominal sclerite VII (instar I): (0) with anterotransverse carina; (1) without anterotransverse carina.
(66)	Principal abdominal tracheal trunks (instars I–III): (0) not protruding from the apex of siphon; (1) protruding backward from the apex of siphon.
(67)	Siphon (instar III): (0) very elongate, ratio LASD/LASV > 3.00; (1) moderately elongate, ratio LASD/LASV = 1.80–2.20; (2) short, ratio LASD/LASV < 1.60.
(68)	Seta AB4 (instar I): (0) short; (1) long.
(69)	Seta AB5 (instar I): (0) short; (1) long.
(70)	Seta AB6 (instar I): (0) short; (1) long.
(71)	Seta AB7 (instar I): (0) present (1) absent.
(72)	Seta AB9 (instar I): (0) inserted dorsolaterally; (1) inserted ventrolaterally.
(73)	Seta AB10 (instar I): (0) hair-like; (1) spine-like.
(74)	Seta AB11 (instar I): (0) hair-like; (1) spine-like.
(75)	Seta AB15 (instar I): (0) present; (1) absent.
(76)	Pore ABa (instar I): (0) present; (1) absent.
(77)	Seta AB3 (instar I): (0) articulated at about level of seta AB2; (1) articulated more apically, distad of seta AB2.
(78)	Secondary ventral setae on siphon (instar III): (0) absent; (1) present.
(79)	Number of primary setae on urogomphus (excluding natatory setae) (instar I): (0) eight; (1) seven.
(80)	Seta UR6 (instar I): (0) long, hair-like; (1) short, spine-like.
(81)	Seta UR8 (instar I): (0) inserted apically on urogomphomere 2; (1) inserted distally on urogomphomere 2; (2) absent.
(82)	Secondary setae on urogomphus (instars II–III): (0) absent; (1) present, short and spine-like; (2) present, predominantly elongate and hair-like.
(83)	Urogomphomere I (instar III): (0) U1/HW < 1.00; (1) U1/HW = 1.40–1.70; (2) U1/HW > 1.80.

larvae; and viii) presence of a very elongate seta FE6 (character 51, Fig. 11).

The strict consensus tree (Fig. 20) resolved *Megaporus* and *Chostonectes* as sister to *Antiporus* although this was not strongly supported. Larvae of both these genera differ from *Antiporus* by: i) the presence of secondary spine-like setae on ventral surface of parietals (character 20) (Fig. 15); ii) absence of elongate spinulae along the lateral margin of prementum in instar I (character 32, Figs. 8–9); and presence of strongly developed ventral marginal spinulae on iii) meso- and metatibiae (character 47), and iv) meso- and metatarsi (character 49, Fig. 16). The close phylogenetic relationship between *Chostonectes* and *Megaporus* reinforces conclusions from previous studies including various data sets (Balke 1995; Hendrich *et al.* 2014; Miller and Bergsten 2014; Toussaint *et al.* 2015). As reasonable as this conclusion might seem, however, it is worth stressing that larvae of *Megaporus* differ strongly from those of *Chostonectes* by several character states. Among these are: i) the presence of a very elongate siphon (character 67, Fig. 18); ii), the more distal articulation of the primary seta AB3 on the siphon (character 77, Fig. 12); and iii) the presence of elongate and hair-like secondary setae on the urogomphi (character 82, Fig. 19), all of which are deemed to represent unique synapomorphies within the known Sternopriscina. In addition to these unique character states, larvae of *Megaporus* also differ from those of *Chostonectes* by the following homoplastic features: i) short antenna (character 06, reversal from the derived condition); ii) distinctly constricted parietals at level of occipital suture in instar III (character 09, Fig. 15); iii) presence

Table 6. Data matrix used for the cladistic analysis. Missing data coded '?'.

Species	00	01	02	03	04	05	06	07	08	09	10	11	12	13	14	15	16	17	18	19	20	21	22	23	24	25	26	27	28	29
Laccornis latens	0	0	0	0	0	0	0	1	0	0	0	1	0	0	1	0	0	0	0	1	1	0	0	1	0	0	0	0	0	1
Antiporus femoralis	1	1	2	1	0	0	1	1	2	0	0	1	0	1	1	1	0	0	0	1	0	1	1	1	0	1	1	1	1	1
Antiporus uncifer	1	1	2	1	0	0	1	1	2	0	0	1	0	1	1	1	0	0	0	1	0	1	1	1	0	1	1	1	1	1
Barretthydrus tibialis	0	0	2	0	0	0	0	0	1	1	0	1	0	1	1	1	0	0	0	1	1	1	1	1	0	1	1	1	1	1
Hydrovatus caraibus	1	0	0	0	1	1	0	0	2	0	0	0	0	0	1	1	1	1	1	0	0	1	0	0	1	1	0	0	0	1
Canthyporus kenyensis	0	0	1	0	0	0	0	1	1	0	0	1	0	0	1	1	1	0	0	0	0	1	0	1	0	0	1	0	1	1
Laccornellus lugubris	0	0	1	0	0	1	0	1	1	0	0	1	0	0	1	1	0	0	0	0	1	1	0	1	0	0	0	0	0	1
Celina parallela	0	0	0	0	0	1	0	1	1	1	1	1	0	1	0	0	0	0	0	1	0	1	0	1	0	0	0	0	0	0
Chostonectes gigas	1	1	2	1	0	0	1	1	2	0	0	1	0	1	1	1	0	0	0	1	1	1	1	1	0	1	1	1	1	1
Paroster darlotensis	1	1	1	1	0	0	0	1	1	0	0	1	1	0	1	1	0	0	0	1	1	1	1	1	0	1	1	1	1	1
Paroster baylyi	0	0	1	0	?	?	0	?	?	0	?	1	0	?	?	?	0	0	0	0	0	1	1	1	0	1	1	1	1	1
Megaporus hamatus	1	1	2	1	0	0	0	1	2	1	0	1	0	1	1	1	0	0	0	1	1	1	1	1	0	1	1	1	1	1

Species	30	31	32	33	34	35	36	37	38	39	40	41	42	43	44	45	46	47	48	49	50	51	52	53	54	55	56	57	58	59
Laccornis latens	0	0	0	0	0	0	0	0	0	0	1	0	0	0	0	0	1	1	1	1	0	1	0	0	0	0	0	0	0	0
Antiporus femoralis	1	1	1	0	0	0	0	0	0	0	0	0	1	1	1	1	1	0	1	0	1	1	1	1	0	1	1	1	1	0
Antiporus uncifer	1	1	1	0	0	0	0	0	0	0	0	0	1	1	1	1	1	0	1	0	1	1	1	1	0	1	1	1	1	0
Barretthydrus tibialis	1	1	0	0	0	0	0	0	0	0	0	0	1	1	1	1	0	0	0	0	1	0	1	1	0	1	1	1	1	0
Hydrovatus caraibus	0	1	0	0	1	1	1	0	1	0	1	1	1	0	0	0	0	0	1	1	1	0	0	0	0	0	0	0	0	1
Canthyporus kenyensis	1	1	1	0	1	0	0	1	1	1	1	0	0	0	0	0	1	1	1	1	0	0	0	0	0	0	0	0	0	0
Laccornellus lugubris	0	1	1	0	1	0	0	1	1	1	1	1	0	0	0	1	1	1	1	1	0	0	1	0	0	0	0	0	0	0
Celina parallela	0	1	0	0	0	1	0	0	0	0	0	1	0	1	0	1	1	0	1	0	1	0	1	0	1	1	1	1	0	0
Chostonectes gigas	1	1	0	0	0	0	0	0	0	0	0	0	1	1	1	1	1	1	1	1	0	1	1	1	0	1	1	1	1	0
Paroster darlotensis	1	1	0	1	0	0	0	2	2	2	0	0	1	1	0	1	0	0	0	0	0	0	1	0	0	1	1	1	0	0
Paroster baylyi	1	1	0	1	0	0	0	2	2	2	0	0	1	1	0	1	0	0	0	0	0	?	1	0	?	1	1	1	0	0
Megaporus hamatus	1	1	0	0	0	0	0	0	0	0	0	0	1	1	1	1	1	1	1	1	1	1	1	1	0	1	1	1	1	0

Species	60	61	62	63	64	65	66	67	68	69	70	71	72	73	74	75	76	77	78	79	80	81	82	83
Laccornis latens	0	1	1	1	0	0	0	2	0	0	0	0	1	0	1	1	0	0	0	0	0	0	0	0
Antiporus femoralis	1	1	1	1	0	1	0	2	0	0	0	0	1	1	1	1	1	0	1	0	0	1	1	2
Antiporus uncifer	1	1	1	1	0	1	0	2	0	0	0	0	1	1	1	1	1	0	0	0	0	1	1	2
Barretthydrus tibialis	1	1	1	1	0	1	0	2	0	0	0	0	1	1	1	1	1	0	0	0	0	1	1	1
Hydrovatus caraibus	0	0	0	0	0	0	0	1	1	1	1	0	0	1	1	1	1	0	1	1	0	2	0	0
Canthyporus kenyensis	0	1	1	0	1	0	0	2	1	1	1	0	1	1	1	1	1	0	0	1	0	2	0	0
Laccornellus lugubris	0	1	1	1	0	0	0	2	1	0	1	0	0	1	1	0	0	0	0	1	0	2	0	0
Celina parallela	0	1	1	1	0	0	1	2	0	0	1	1	1	0	0	1	1	0	1	0	1	0	0	0
Chostonectes gigas	1	1	1	1	0	1	0	1	0	0	0	0	1	1	1	1	1	0	0	0	0	1	1	2
Paroster darlotensis	1	1	1	1	0	1	0	2	0	0	0	0	1	1	1	1	1	0	0	0	0	1	1	2
Paroster baylyi	?	1	1	1	?	?	0	2	?	?	?	?	?	?	?	?	?	0	0	?	?	?	1	2
Megaporus hamatus	1	1	1	1	0	1	0	0	1	0	0	0	1	1	1	1	1	1	0	0	0	1	2	2

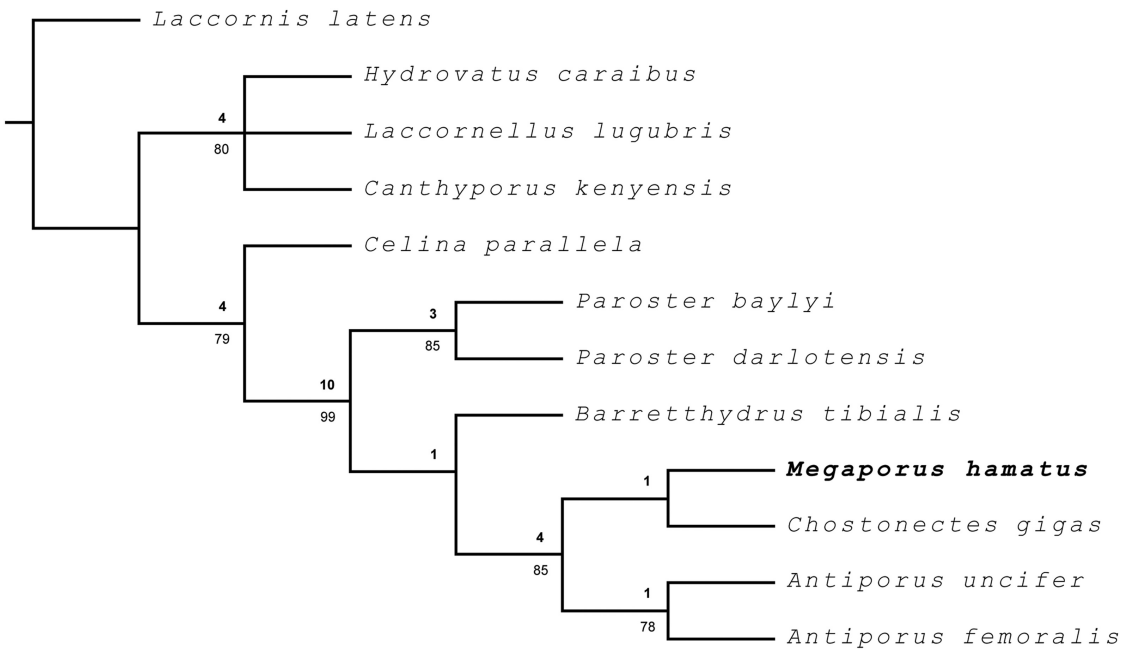

Fig. 20. Strict consensus cladogram obtained from the cladistic analysis of 12 terminal taxa of Hydroporinae with Bremer support values indicated above branches and Bootstrap values higher than 50 indicated below branches.

of compound secondary femoral setae along the ventral margin (character 50, Fig. 16); and iv) presence of an elongate primary seta AB4 (character 68, Fig. 12). Such a strong dissimilarity between the larvae of two apparently closely related taxa reinforces the importance of expanding the set of characters to include information-rich larval traits when inferring insect phylogenetic relationships.

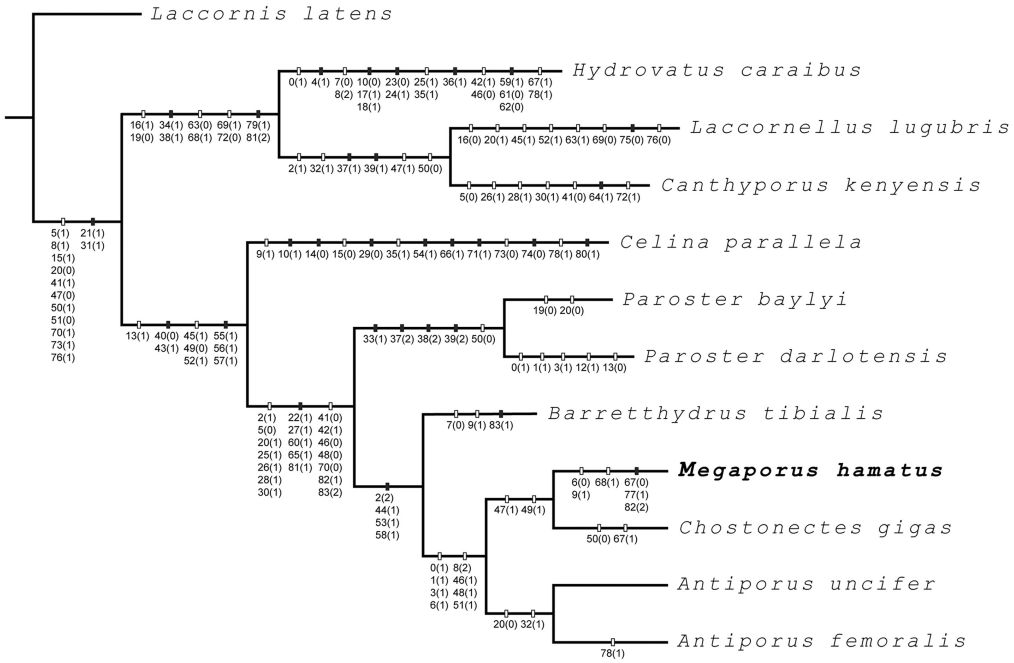

Fig. 21. One of the most parsimonious trees obtained from the cladistic analysis of 12 terminal taxa of Hydroporinae, with selected character changes mapped for each clade (using ACCTRAN optimization). Solid rectangles indicate unique character state transformations; open rectangles indicate homoplasious character state transformations.

Acknowledgments

The work of M. C. Michat was supported by ANPCyT under Grant PICT-2014-0853, and by University of Buenos Aires under Grant UBACyT-20020150100170BA.

References Cited

Alarie, Y. 1991. Primary setae and pores on the cephalic capsule and head appendages of larval Hydroporinae (Coleoptera: Dytiscidae). Canadian Journal of Zoology 69: 2255–2265.

Alarie, Y., and P.-P. Harper. 1990. Primary setae and pores on the last abdominal segment and the urogomphi of larval Hydroporinae (Coleoptera: Adephaga: Dytiscidae), with notes on other dytiscid larvae. Canadian Journal of Zoology 68: 368–374.

Alarie, Y., P.-P. Harper, and A. Maire. 1990. Primary setae and pores on legs of larvae of Nearctic Hydroporinae (Coleoptera: Dytiscidae). Quaestiones Entomologicae 26: 199–210.

Alarie, Y., and M. C. Michat. 2007a. Primary setae and pores on the maxilla of larvae of the subfamily Hydroporinae (Coleoptera: Adephaga: Dytiscidae): ground plan pattern reconsidered. The Coleopterists Bulletin 61: 310–317.

Alarie, Y., and M. C. Michat. 2007b. Phylogenetic analysis of Hydroporinae (Coleoptera: Dytiscidae) based on larval morphology, with description of first instar of *Laccornellus lugubris.* Annals of the Entomological Society of America 100: 655–665.

Alarie, Y., M. C. Michat, L. Hendrich, and C. H. S. Watts. 2018. Larval description and phylogenetic placement of the Australian endemic genus *Barretthydrus* Lea, 1927 (Coleoptera: Dytiscidae: Hydroporinae: Hydroporini: Sternopriscina). The Coleopterists Bulletin 72: 639–661.

Alarie, Y., M. C. Michat, L. Hendrich, and C. H. S. Watts. 2019. Larval morphology of the Australian radiation Sternopriscina (Coleoptera: Dytiscidae, Hydroporinae): description and phylogenetic placement of the genus *Chostonectes* Sharp, 1882. Aquatic Insects 40: 328–354. DOI: 10.1080/01650424.2019.1610570.

Alarie, Y., M. C. Michat, and C. H. S. Watts. 2009. Larval morphology of *Paroster* Sharp, 1882 (Coleoptera: Dytiscidae: Hydroporinae): reinforcement of the hypothesis of monophyletic origin and discussion of phenotypic accommodation to a hypogaeic environment. Zootaxa 2274: 1–44.

Alarie, Y., and C. H. S. Watts. 2004. Larvae of the genus *Antiporus* (Coleoptera: Dytiscidae) and phylogenetic implications. Invertebrate Systematics 18: 523–546.

Balke, M. 1995. The Hydroporini (Coleoptera: Dytiscidae: Hydroporinae) of New Guinea: Systematics, distribution and origin of the fauna. Invertebrate Taxonomy 9: 1009–1019.

Bertrand, H. 1972. Larves et nymphes des Coléoptères aquatiques du globe. F. Paillart, Paris, 804 pp.

Goloboff, P. A., J. Farris, and K. Nixon. 2008. TNT, a free program for phylogenetic analysis. Cladistics 24: 774–786.

Hendrich, L., E. F. A. Toussaint, and M. Balke. 2014. A new genus of Hydroporini from south-western Australia (Coleoptera, Dytiscidae). Spixiana 37: 103–109.

Kitching, I. J., P. L. Forey, C. J. Humphries, and D. M. Williams. 1998. Cladistics. The Theory and Practice of Parsimony Analysis. Systematic Association Publications, 11. Oxford University Press, New York, NY, xii + 228 pp.

Lawrence, J. F. 1991. Order Coleoptera [pp. 144–658]. *In*: Immature Insects, Volume 2 (F. W. Stehr, editor). Kendall Hunt Publishing Co., Dubuque, IA, xvi + 975 pp.

Michat, M. C., Y. Alarie, P. L. M. Torres, and Y. Megna. 2007. Larval morphology of the diving beetle *Celina* and the phylogeny of ancestral hydroporines (Coleoptera: Dytiscidae: Hydroporinae). Invertebrate Systematics 21: 239–254.

Miller, K. B., G. W. Wolfe, and O. Biström. 2006. The phylogeny of the Hydroporinae and classification of the genus *Peschetius* Guignot, 1942 (Coleoptera: Dytiscidae). Insect Systematics and Evolution 37: 1–23.

Miller, K. B., and J. Bergsten. 2014. The phylogeny and classification of predaceous diving beetles [pp. 49–172]. *In*: Ecology, Systematics and the Natural History of Predaceous Diving Beetles (Coleoptera: Dytiscidae) (D. A. Yee, editor). Springer, New York, NY, xviii + 468 pp.

Miller, K. B., and J. Bergsten. 2016. Diving Beetles of the World. Systematics and Biology of the Dytiscidae. Johns Hopkins University Press, Baltimore, MD, ix + 320 pp.

Nilsson, A. N., and J. Hájek. 2019. A world catalogue of the family Dytiscidae, or the diving beetles (Coleoptera, Adephaga), Version 1.I.2019. Distributed as a PDF file via Internet. waterbeetles.eu/documents/

W_CAT_Dytiscidae_2019.pdf (accessed 7 June 2019).

Roughley, R. E., and G. W. Wolfe. 1987. *Laccornellus* (Coleoptera: Dytiscidae), a new hydroporine genus from austral South America. Canadian Journal of Zoology 65: 1346–1353.

Toussaint, E. F. A., F. L. Condamine, O. Hawlitschek, C. H. S. Watts, N. Porch, L. Hendrich, and M. Balke. 2015. Unveiling the diversification dynamics of Australasian predaceous diving beetles in the Cenozoic. Systematic Biology 64: 3–24.

Watts, C. H. S. 1978. A revision of the Australian Dytiscidae (Coleoptera). Australian Journal of Zoology Supplemental Series 57: 1–166.

(Received 29 June 2019; accepted 15 January 2020. Publication date 25 March 2020.)